

Large grain size obtained by substrate directly heating for YBCO epitaxial films

Kebin Li(李珂彬), Yifei Zhang(张一飞), Tong Zhang(张同), Shuguang Yi(易曙光), Shi-Peng Zhang(张世鹏), Quan-Ming Gao(高全明), and Shan-Dong Li(李山东)

Citatio: Chin. Phys. B, 2025, 34 (**9**): 097403. DOI: 10.1088/1674-1056/add4fc
http://cpb.iphy.ac.cn; http://iopscience.iop.org/cpb

What follows is a list of articles you may be interested in

Optimization of large-area $YBa_2Cu_3O_{7-\delta}$ thin films by pulsed laser deposition for planar microwave devices

Pei-Yu Xiong(熊沛雨), Fu-Cong Chen(陈赋聪), Zhong-Pei Feng(冯中沛), Jing-Ting Yang(杨景婷), Yu-Dong Xia(夏钰东), Yue-Feng Yuan(袁跃峰), Xu Wang(王旭), Jie Yuan(袁洁), Yun Wu(吴云), Jing Shi(石兢), and Kui Jin(金魁)
Chin. Phys. B, 2023, 32 (**7**): 077402. DOI: 10.1088/1674-1056/accb4d

Enhancing superconductivity of ultrathin $YBa_2Cu_3O_{7-\delta}$ films by capping non-superconducting oxides

Hai Bo(薄海), Tianshuang Ren(任天爽), Zheng Chen(陈峥), Meng Zhang(张蒙), Yanwu Xie(谢燕武)
Chin. Phys. B, 2019, 28 (**6**): 067402. DOI: 10.1088/1674-1056/28/6/067402

Strongly enhanced flux pinning in the $YBa_2Cu_3O_{7-X}$ films with the co-doping of $BaTiO_3$ nanorod and Y_2O_3 nanoparticles at 65 K

Wang Hong-Yan (王洪艳), Ding Fa-Zhu (丁发柱), Gu Hong-Wei (古宏伟), Zhang Teng (张腾)
Chin. Phys. B, 2015, 24 (**9**): 097401. DOI: 10.1088/1674-1056/24/9/097401

Effects of thickness on superconducting properties and structures of Y_2O_3/BZO-doped MOD-YBCO films

Ding Fa-Zhu (丁发柱), Gu Hong-Wei (古宏伟), Wang Hong-Yan (王洪艳), Zhang Hui-Liang (张慧亮), Zhang Teng (张腾), Qu Fei (屈飞), Dong Ze-Bin (董泽斌), Zhou Wei-Wei (周微微)
Chin. Phys. B, 2015, 24 (**5**): 057401. DOI: 10.1088/1674-1056/24/5/057401

Fabrication and properties of high performance $YBa_2Cu_3O_{7-\delta}$ radio frequency SQUIDs with step-edge Josephson junctions

Liu Zheng-Hao (刘政豪), Wei Yu-Ke (魏玉科), Wang Da (王达), Zhang Chen (张琛), Ma Ping (马平), Wang Yue (王越)
Chin. Phys. B, 2014, 23 (**9**): 097401. DOI: 10.1088/1674-1056/23/9/097401

Large grain size obtained by substrate directly heating for YBCO epitaxial films

Kebin Li(李珂彬), Yifei Zhang(张一飞), Tong Zhang(张同), Shuguang Yi(易曙光), Shi-Peng Zhang(张世鹏), Quan-Ming Gao(高全明), and Shan-Dong Li(李山东)†

Shandong Key Laboratory of Advanced Packaging, System Integration and Applications, College of Electronics and Information, Qingdao University, Qingdao 266071, *China*

(Received 28 February 2025; revised manuscript received 22 April 2025; accepted manuscript online 7 May 2025)

It is very important for high temperature superconducting electronic devices to increase the grain size of YBCO epitaxial films because it can effectively reduce the defects and improve the probability of successful preparation of Josephson junction. In this study, $YBa_2Cu_3O_{7-\delta}$ (YBCO) films with grain size in excess of 1.5 μm were successfully prepared by the directly heating $SrTiO_3$ substrates coated by SiC on their back. Interestingly, the grain size of YBCO film is enhanced greatly by this directly heating method, and the critical temperature T_C and critical current density J_C of YBCO films are as high as 91.5 K and 3.5 MA/cm^2, respectively. Compared with the traditional indirect heating method, which involves applying silver paste and then using a heat soaking block (*e.g.* Inconel 600), this direct heating method effectively enhances the grain size of YBCO film and the possibility of successful preparation of Josephson junction.

Keywords: YBCO film, grain size, critical temperature, critical current density

PACS: 74.25.–q, 74.25.Sv, 74.78.–w, 81.15.Fg

DOI: 10.1088/1674-1056/add4fc **CSTR:** 32038.14.CPB.add4fc

1. Introduction

In the wave of the rapid development of modern technology, superconducting quantum interference devices (SQUIDs) shine brightly in numerous fields due to their excellent performance. In the biomedical field, they can accurately detect the weak magnetic signals within the body, facilitating the diagnosis of early stage diseases and bringing hope for the innovation of medical technology.[1–3] In geophysical exploration, they can be used to detect the distribution of mineral resources deep underground and the subtle changes in geological structures, providing crucial data for resource development and geological research.[4–7] In the field of quantum computing, they are expected to become the core components for constructing high-performance qubits, driving computing power to new heights.[8–10]

In the fabrication of SQUIDs, the Josephson junction represents the most critical component, whose performance is fundamentally dependent on the quality of the YBCO thin films.[11,12] Meanwhile, YBCO thin films also have extensive applications in microwave devices and other fields.[13,14] High quality YBCO films are typically prepared using pulsed laser deposition (PLD), a process that necessitates heating the substrate to temperatures ranging between 760 °C and 850 °C, with specific temperatures varying according to the substrate material.[13,15] The surface resistance of YBCO exhibits a strong dependence on grain boundary density, with experimental studies demonstrating that enlarging the grain size in YBCO thin films is required to reduce these defects.[16,17] In the fabrication of SQUID loops using focused ion beam (FIB) technology, grain boundary regions exhibit significant sensitivity to ion beam irradiation. Compared to grain interiors, grain boundaries are more susceptible to FIB-induced damage. Therefore, employing large-grained film materials can reduce the grain boundary density per unit area, thereby minimizing the damage generated during FIB etching and significantly enhancing the performance of Josephson junctions as well as the processing yield of SQUID devices.[18] Regarding the meandering structures caused by bicrystal grain boundary defects, increased grain size enhances grain boundary positioning accuracy.[19] Jun HyungLim noted that as the grain size increases, YBCO films become denser, leading to a significant enhancement in the critical current density.[20] Consequently, strategies for enlarging grain size have become a prominent research focus.[21] For example, significant progress has been achieved in controlling YBCO film grain structures through deposition temperature adjustment and in depositing on YSZ single crystal fibers. However, these methodologies still face dual technical challenges: either the grain size remains suboptimal or the assistance of a CeO_2 buffer layer is required.[16,22] Generally, heating is achieved by applying silver paste to the back of the substrate, which is then affixed to a thermally conductive block. However, this indirect heating approach presents several significant limitations. Firstly, it is challenging to maintain the optimal growth temperature for YBCO films due to inconsistencies in the thickness of the applied silver paste. Secondly, non-uniform distribution of the silver

†Corresponding author. E-mail: dylsd007@163.com

© 2025 Chinese Physical Society and IOP Publishing Ltd. All rights, including for text and data mining, AI training, and similar technologies, are reserved.

paste can lead to uneven film growth, thereby compromising the film's performance. Additionally, this method is associated with substantial heat loss during the film growth process, which inhibits the formation of YBCO films with large grain sizes.[23–25]

To overcome these limitations, this study proposes an innovative heating technique. In this method, a layer of silicon carbide (SiC) is deposited onto the back of the substrate via magnetron sputtering, followed by direct infrared heating of the substrate. This approach has successfully enabled the fabrication of large-area YBCO films with superior properties. Characterization results demonstrate that the fabricated films exhibit excellent superconducting performances with a critical temperature (T_C) of 91.5 K and a critical current density (J_C) of 3.5 MA/cm^2. The non-doped YBCO thin films mentioned in the paper by Shipulin exhibit a J_C of 1.4 MA/cm^2,[26] while the YBCO films prepared via Fluorine-free MOCSD method by Rasti achieve a J_C of 2 MA/cm^2.[27] Compared to the conventional heating method using silver paste, the proposed approach provides more sufficient energy for film growth, enabling the fabrication of high performance YBCO films with large grain size of 1.5 μm. Shimizu fabricated YBCO thin films with a grain size of 775 nm on STO substrates,[28] while Rasti prepared YBCO films via Fluorine-free MOCSD method achieving a grain size about 200 nm–300 nm.[27] This method eliminates the manual application of silver paste, resulting in a more stable and reproducible preparation process while ensuring excellent film uniformity. Furthermore, by avoiding the repeated procurement of silver paste, it circumvents potential experimental inconsistencies caused by variations in the quality of silver paste. These advantages establish a critical foundation for the preparation of high quality Josephson junctions.

2. Experiment

2.1. Samples preparation

In this experiment, we prepared two YBCO thin films, namely, S1 and S2. Both were fabricated on [001]-oriented $SrTiO_3$ substrates using a customized pulsed laser deposition system (TSST company), but using different heating methods. A KrF excimer laser with a wavelength of 248 nm, a pulse fluence of 2 J/cm^2, and a repetition rate of 1 Hz was used. During the deposition, the distance between the sample and the target was controlled at 55 mm. With the help of a laser heater, the sample temperature was controlled at 800 °C and maintained under an oxygen pressure of 25 Pa. After the deposition was completed, the sample temperature was decreased to 500 °C at a cooling rate of 5 °C per minute. Finally, a heat-preservation treatment was carried out for 4 hours under an oxygen pressure of 80 kPa. The thickness of both films was 40 nm.

During the preparation of samples S1 and S2, different heating methods were adopted for them. For sample S1, an indirect heating strategy was employed. Specifically, silver paste was evenly smeared on the back of the substrate, and then the substrate was closely attached to a 4-mm-thick Inconel soaking block and heated to 800 °C. For sample S2, a new heating method was employed. An SiC heat-soaking layer with a thickness of around 50 μm was deposited on the back of the $SrTiO_3$ substrate by magnetron sputtering to further enhance the heat-absorption capacity of the substrate. Finally, the substrate was directly heated to 800 °C by a laser heater. A comparison diagram of these two heating methods is shown in Fig. 1.

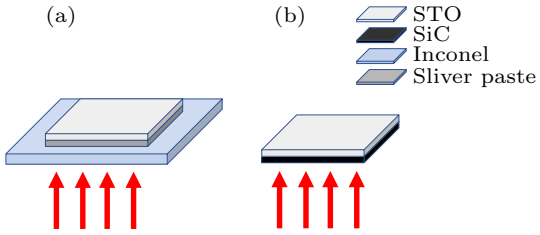


Fig. 1. Schematic diagram of substrate heating method. (a) Silver paste on Inconel 600, (b) silicon carbide (SiC) coated on $SrTiO_3$ substrate directly.

2.2. Characterization of $YBa_2Cu_3O_{7-\delta}$ films

The surface morphology of the thin films was observed by scanning electron microscopy (SEM), and atomic force microscopy (AFM). The epitaxy and atomic arrangement of the films were observed in cross-section samples by spherical aberration correction transmission electron microscopy (Cs-TEM). The x-ray diffraction (XRD) with a general area detector diffraction system was used to characterize the phase and texture of the films. The critical temperature and critical current density of the two samples were measured by the standard four-probe method after fabricating the microstrip of YBCO thin films with a width of 7 μm–10 μm by photolithography and Ar^+ etching.

3. Result and discussion

Figures 2(a) and 2(c) show the four-probe resistance measurements as a function of temperature conducted on the microstrips with different widths for the two thin films of S1 and S2, respectively. Both films exhibit superconducting transition onset (T_{onset}) well above the liquid nitrogen temperature. For sample S1, it was between 88 K and 91 K, while for sample S2, it was between 91 K and 92 K. It can be seen that the onset transition temperature of S2 is slightly higher than that of S1. The critical temperatures of the four microstrips of S1 and S2 can be obtained by performing differential calculations on the R–T curves and taking the point with the largest derivative as the critical temperature (T_C), which are respectively between 87 K–89 K and 91 K–91.5 K. The transition width ΔT of sample S1 ranges from 2.6 K to 5.3 K, while that of S2 is narrowed to 1.4 K–3.8 K, demonstrating the latter's superior crystalline uniformity and enhanced structural

integrity.[29] The two samples exhibit metallic behavior above T_{onset}.[30] The normal-state resistances of the four microstrips of the two samples comply with the negative correlation rule between the line width and the resistance. However, at room temperature (300 K), S2 demonstrated a significantly lower resistivity compared to S1.

Meanwhile, it should be noted that there are significant differences in the critical current characteristics between S1 and S2. The critical current (I_C) of the two samples were measured at the temperature of liquid nitrogen (77 K), and the measurement results are shown in Figs. 2(b) and 2(d). The I_C of the samples increases as the line width increases, and each curve is symmetrical about the origin. The I_C and the calculated critical current densities (J_C) of the two samples are shown in Table 1. As can be seen from Table 1, the J_C of sample S1 is between 2 MA/cm^2–2.5 MA/cm^2, while that of sample S2 is between 3 MA/cm^2–3.8 MA/cm^2.[31] It can be seen that the superconducting properties of sample S2 prepared by the direct heating method using SiC coating layer are obviously superior to those of sample S1 prepared by the indirect heating method with silver pasted. In addition, we also conducted XRD tests on the two samples.

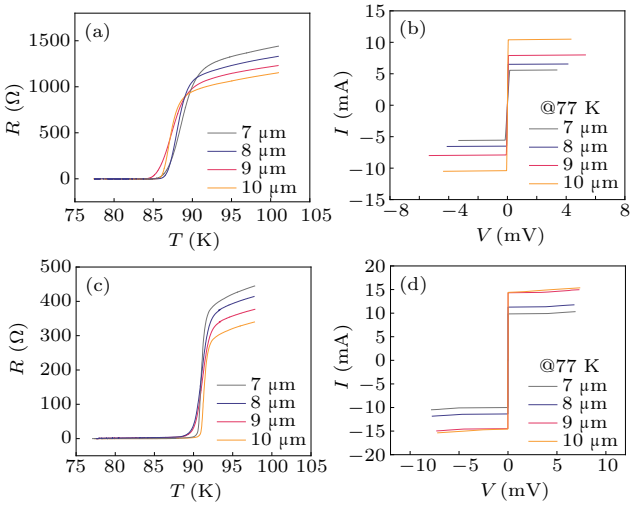


Fig. 2. Resistance and temperature curves of microstrip lines with different widths for (a) S1 and (c) S2. The *I*–*V* characteristics of microstrip lines with different widths at 77 K for (b) S1 and (d) S2.

Table 1. Comparisons of superconducting performance parameters of different micro-strips of two samples S1 and S2.

Micro-strips (μm)	I_C (mA)	J_C (MA/cm^2)	T_C (K)	T_{oneset} (K)	ΔT (K)	Resistivity @300 K/Ω·m
S1-7	5.5	1.964	88.7	90.9	4.5	1.273×10^{-6}
S1-8	6.6	2.063	88.3	89.6	3.6	1.254×10^{-6}
S1-9	7.6	2.111	87.4	89.5	5.3	1.239×10^{-6}
S1-10	10.2	2.55	87.5	88.3	2.6	1.208×10^{-6}
S2-7	9.4	3.357	91.0	91.7	1.8	4.566×10^{-7}
S2-8	10.9	3.406	90.9	92.2	3.8	4.514×10^{-7}
S2-9	13.9	3.861	91.1	92.2	3.8	4.421×10^{-7}
S2-10	14.4	3.6	91.4	92.1	1.4	4.487×10^{-7}

The XRD patterns at room temperatures for two samples are shown in Fig. 3 from 10° to 70° of 2θ angle. In Fig. 3(a), the blue parts on the abscissa correspond to the (00l) thin film peaks of YBCO. It can be seen that both samples grow only in the (00l) direction, which indicates that both samples are composed of a single $Y_1Ba_2Cu_3$ phase.[32] We performed rocking scans on the (005) peaks of samples S1 and S2 and calculated the full-width at half maximum (FWHM). It can be observed that the full-width at half maximum of both samples S1 and S2 is less than 0.2°, which indicates that the crystal structure quality of the thin films is good and the crystal grains are highly aligned along the *c*-axis.[22] Moreover, the full-width at half maximum of sample S2 is much smaller than that of sample S1, suggesting that the grain size of sample S2 is larger.[33] The YBCO (103) plane was used to measure the in-plane orientations (φ-scan). The φ-scans for the films in Fig. 3(b) show sharp reflections every 90° for all substrates, indicating a 4-fold symmetry due to epitaxial growth.[34]

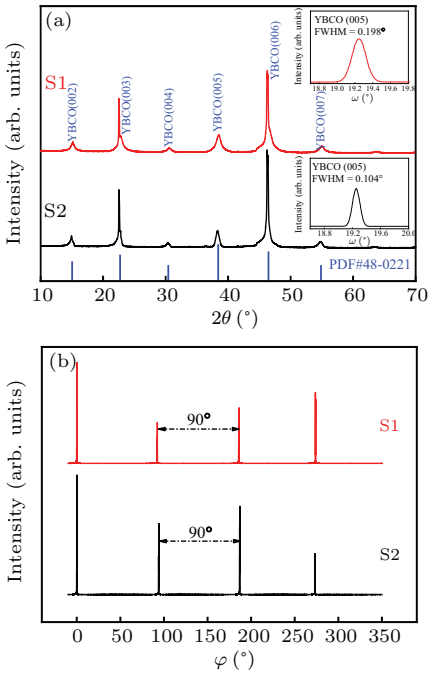


Fig. 3. XRD characterization of YBCO films deposited on $SrTiO_3$ substrates. (a) The θ–2θ diffraction pattern and rocking curve of YBCO (005) peak. (b) The φ-scan result of YBCO (103) peaks.

The AFM and SEM images of samples S1 and S2 are shown in Fig. 4. Figures 4(a) and 4(c) are the AFM images of samples S1 and S2 with a size of 5 μm×5 μm, respectively. As shown in the figures, the grain size of sample S1 is around 0.6 μm, while that of sample S2 is 1.5 μm. By comparing the average surface roughness (R_a) of the 5 μm×5 μm areas of the two samples, we found that the R_a value of sample S1 is 5.612 nm, and that of sample S2 is 2.984 nm. As shown in the SEM images, the grain size of sample S2 is significantly larger than that of sample S1, with denser interconnections between grains. Comparative analysis of AFM and SEM images between the two samples demonstrates that the direct heating method effectively enhances grain growth, resulting in significantly enlarged grain dimensions in the YBCO thin film. Based on the correlation analysis between the microstructure and superconducting properties of the two samples, S2 exhibited significant grain coarsening compared to S1, leading to a reduced grain boundary density. Moreover, weak links tend to form at grain boundaries, which significantly reduce the J_C of YBCO film. This mechanism explains the enhanced J_C of S2, with an average value of 3.5 MA/cm^2, representing a ∼ 60% improvement over S1. These results are consistent with the conclusions reported by Ohshima.[35]

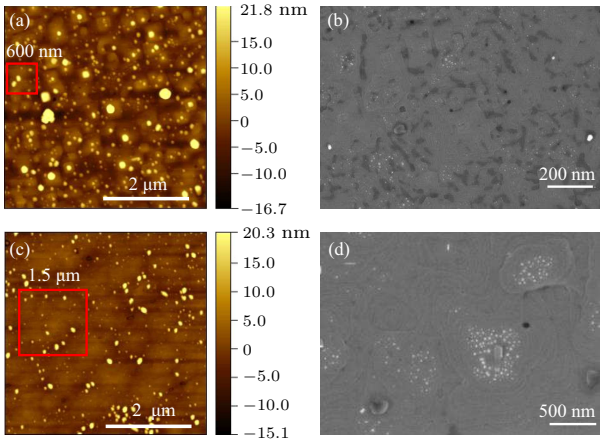


Fig. 4. The AFM image of the 5 μm×5 μm area for (a) S1, (c) S2. The SEM images at the same magnification of S1 (b) and S2 (d).

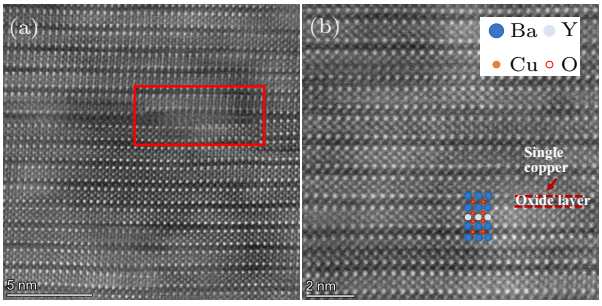


Fig. 5. The STEM–HADDF image of YBCO films grown on $SrTiO_3$ substrate for (a) S1 and (b) S2.

In addition, Cs–TEM analysis was performed on both S1 and S2 samples, with the results presented in Fig. 5. The region highlighted by the red rectangle in Fig. 5(a) reveals distinct partial dislocations in S1, while in contrast, no significant lattice defects were observed in S2. Moreover, only the single copper oxide layer exists in S1, and there is no presence of the double copper oxide layer (YBCO-124 phase).[36] This indicates that the direct heating method with SiC coating on the back can effectively prepare high quality YBCO thin films.

As shown above, we have prepared high-quality YBCO films with a grain size of over 1.5 μm through the directly heating method with SiC coated on the back of the substrate. The large grain size obtained by directly heating method can be attributed to the high heat flux which can provide sufficient growth energy for YBCO films. The growth mode of YBCO films depends on the lattice matching degree between the substrate and YBCO. There are two modes: the Stranski–Krastanov mode and the Volmer–Weber mode. The YBCO grows in the Stranski–Krastanov mode on the lattice-matched $NdGaO_3$, while on less lattice-matched $SrTiO_3$, the YBCO grows in the Volmer–Weber mode.[37,38] In this growth mode, the deposited atoms adsorbed on the substrate surface migrate on the substrate surface and combine to form atomic clusters or even stable nuclei. Each stable YBCO nucleus grows into islands in three-dimensional (3D) directions by capturing adsorbed atoms or directly accepting incident atoms. During the growth process, the islands meet and merge into larger islands, and then form a network-like thin film, which gradually grows into a complete thin film. The processes of nuclei capturing adatoms and island growth require stable energy input. The measured thermal conductivity of SiC is approximately 140 W/(m·K), while that of Inconel 600 stainless steel soaking block is lower than 15 W/(m·K). The huge difference in thermal conductivity causes a huge difference in heat flux, so that the SiC direct-heated sample has sufficient heat to provide growth power, and then achieve larger grains. As a result, sample S2 exhibits larger grains compared to sample S1. Meanwhile, under the influence of the backside-sputtered SiC layer, vertically oriented thermal conduction channels form at the substrate-film interface, enabling rapid dissipation of localized thermal fluctuations of adatoms during deposition, thereby maintaining a more uniform lateral temperature gradient. This quasi-steady-state thermal environment significantly extends the surface diffusion length, which promotes preferential migration of incident atoms to the edges of preexisting 3D islands rather than forming new nuclei. Consequently, the critical island size shifts toward larger dimensions, ultimately facilitating the coalescence of millimeter-scale single-crystal domains.

To verify the critical role of thermal conductivity in grain

size enlargement, two directly heated comparative samples were fabricated under identical processing conditions (with thermal interface materials being the sole variable from S1 and S2). Specifically, S3 was prepared by back-coated with 25 W/(m·K) silver paste, while S4 employed 75 W/(m·K) platinum paste as the back-coated layer. Comparative analysis of AFM images in Fig. 6 reveals that S3 exhibits grain sizes around 700 nm, whereas S4 with enhanced thermal conductivity demonstrates significantly enlarged grains approaching 900 nm. The parameter comparisons in Table 2 across all four samples further confirm that increased thermal conductivity substantially promotes grain growth, demonstrating a distinct positive correlation between these two parameters.

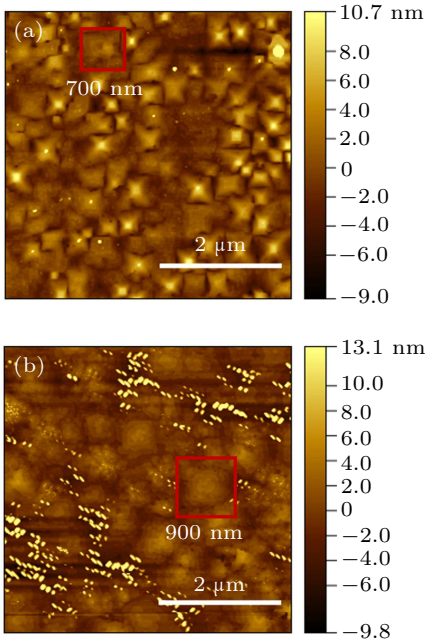


Fig. 6. The AFM image of the 5 μm×5 μm area for (a) S3, (b) S4.

Table 2. Comparative analysis of thermal conductivity and grain size in fabricated samples.

Sample	Thermal conductive material	Thermal conductivity (W/(m·K))	Grain size (nm)
S1	inconel 600	15	600
S2	SiC	140	1500
S3	silver paste	25	700
S4	platinum paste	75	90

4. Conclusion

In this study, the YBCO film samples were prepared using two different heating methods: using heat-soaking block (S1) and SiC directly heating (S2), respectively. Experimental results indicate that the YBCO films prepared by both methods exhibit excellent *c*-axis orientation properties. However, the T_C and J_C of sample S2 are evidently higher than those of sample S1. This difference is primarily attributed to the larger grain size and closer intergranular connections in sample S2. For sample S2, energy loss during the heating process is significantly reduced. This provides more sufficient growth energy for the YBCO films, promoting the formation of small islands and their subsequent coalescence into larger islands, thereby enabling the grain diameter of S2 in excess of 1.5 μm.

Acknowledgements

Project supported by the National Key Research and Development Program of China (Grant No. 2023YFF0720500), the State Key Program of the National Natural Science Foundation of China (Grant No. U22A2019), and the National Key Project (Grant No. 22-05-CXZX-04-03-15).

References

[1] Tolpygo S K, Bolkhovsky V, Weir T J, Wynn A, Oates D E, Johnson L M and Gouker M A 2016 *IEEE Transactions on Applied Superconductivity* **26** 1
[2] Yang H C, Wu T Y, Horng H E, Wu C C, Yang S Y, Liao S H, Wu C H, Jeng J T, Chen J C, Chen K L and Chen M J 2006 *Superconductor Science and Technology* **19** S297
[3] Zhang X, Ying L, Niu M, Zhang H, Liu H, Wu Y, Xu W, Chen L, Shao Y, Liang T, Ma L, Jin H, Xie H, Gao Y, Sun H, Ren J, Peng W, Maezawa M and Wang Z 2021 *IEEE Transactions on Applied Superconductivity* **31** 1
[4] Schmelz M, Zakosarenko V, Chwala A, Schönau T, Stolz R, Anders S, Linzen S and Meyer H G 2016 *IEEE Transactions on Applied Superconductivity* **26** 1
[5] Hato T, Tsukamoto A, Adachi S, Oshikubo Y, Watanabe H, Ishikawa H, Sugisaki M, Arai E and Tanabe K 2013 *Superconductor Science and Technology* **26** 115003
[6] Song Z, Dai H, Rong L, Dong H, Wu J, Qiu L, Zhang G, Wang Y, Tao Q, Pei Y, Zhang S and Xie X 2019 *IEEE Transactions on Applied Superconductivity* **29** 1
[7] Rong L, Bao S, Wu J, Zhang G, Qiu L, Zhang S, Wang Y, Dong H, Pei Y and Xie X 2019 *IEEE Transactions on Applied Superconductivity* **29** 1
[8] Xue Z Y, Dong P, Yi Y M and Cao Z L 2007 *Physica C* **458** 58
[9] Campbell D L, Shim Y P, Kannan B, Winik R, Kim D K, Melville A, Niedzielski B M, Yoder J L, Tahan C, Gustavsson S and Oliver W D 2020 *Phys. Rev. X* **10** 041051
[10] Shirai S, Okubo Y, Matsuura K, Osada A, Nakamura Y and Noguchi A 2023 *Phys. Rev. Lett.* **130** 260601
[11] Jaklevic R C, Lambe J, Silver A H and Mercereau J E 1964 *Phys. Rev. Lett.* **12** 159
[12] Faley M I, Dammers J, Maslennikov Y V, Schneiderman J F, Winkler D, Koshelets V P, Shah N J and Dunin-Borkowski R E 2017 *Superconductor Science and Technology* **30** 083001
[13] Xiong P Y, Chen F C, Feng Z P, Yang J T, Xia Y D, Yuan Y F, Wang X, Yuan J, Wu Y and Shi J 2023 *Chin. Phys. B* **32** 077402
[14] Zhang Y F, Zhang S N, Liu J X, Yang F, Li C S, Li J F and Zhang P X 2024 *Chin. Phys. Lett.* **41** 117402
[15] QueraltÓ A, Sieger M, Gupta K, Meledin A, Barusco P, Saltarelli L, de Palau M, Granados X, Obradors X and Puig T 2022 *Superconductor Science and Technology* **36** 025003
[16] Mukaida M, Sato S, Takano Y, Kusunoki M and Ohshima S 2002 *Physica C* **378–381** 1232
[17] Cardwell D A 1998 *Materials Science and Engineering: B* **53** 1
[18] Lee S G, Hong S H, Seong W K and Kang W N 2009 *Superconductor Science and Technology* **22** 064009
[19] Zhang X, Miller D and Talvacchio J 1996 *Journal of Materials Research* **11** 2440
[20] Lim J H, Jang S H, Joo J, Kim H, Lee H G, Hong G W and Kim C J 2006 *Superconductor Science and Technology* **19** 306
[21] Aslan Çataltepe Ö, Güven Özdemir Z and Onbaşli Ü 2013 *Physica C* **491** 59

[22] Snigirev O, Chukharkin M, Porokhov N, Rusanov S Y, Kashin V V, Tsvetkov V B, Kalabukhov A and Winkler D 2014 *J. Phys.: Conf. Ser.* **507** 022033
[23] Nishioka T, Amemiya N, Jiang Z, Iijima Y, Saitoh T, Yamada M and Shiohara Y 2004 *Physica C* **412–414** 992
[24] Lee J B, Lee S U, Kim S S, Kim B J, Kim H J, Yoo Y S, Kim J G, Hong G W and Lee H G 2009 *Physica C* **469** 952
[25] Din F U, Shaari A H, Kien C S, Talib Z A, Din A U and Pah L K 2018 *J. Phys.: Conf. Ser.* **1082** 012024
[26] Shipulin I A, Anna Thomas A, Holleis S, Eisterer M, Nielsch K and Hühne R 2022 *Materials* **15** 5354
[27] Rasti M and Mohammadizadeh M R 2020 *IEEE Transactions on Applied Superconductivity* **30** 1
[28] Shimizu Y, Takashima H, Yoshida Y and Furuse M 2018 *IEEE Transactions on Applied Superconductivity* **28** 1
[29] Dai X H, Song J M, Zhao L, Wang Y L, Zhao H D and Liu B T 2020 *Appl. Phys. A* **126** 895
[30] Arlina A, Halim S A, Kechik M M A and Chen S K 2015 *J. Alloys Compd.* **645** 269
[31] Paturi P, Irjala M and Huhtinen H 2008 *J. Appl. Phys.* **103** 123907
[32] Malisa A 2005 *Annalen der Physik* **517** 533
[33] Gogova D, Tran D Q, Stanishev V, Jokubavicius V, Vines L, Schubert M, Yakimova R, Paskov P P and Darakchieva V 2024 *J. Vac. Sci. Technol. A* **42** 022708
[34] Du J, Gnanarajan S and Bendavid A 2004 *Physica C* **400** 143
[35] Ohshima S, Kusunoki M, Mukaida M, Suzuki T, Chibai K, Inadomaru M and Takano Y 2001 *IEEE Transactions on Applied Superconductivity* **11** 3493
[36] Liu X, He Y, Li P, Li W, Wang Y and Zhou M 2024 *Physica C* **623** 1354551
[37] Wu K H, Wang R C, Chen S P, Lin H C, Juang J Y, Uen T M and Gou Y S 1996 *Appl. Phys. Lett.* **69** 421
[38] Miyazawa S, Sasaura M and Mukaida M 1993 *Journal of Crystal Growth* **128** 704